Article:
Bux, J, Peakall, J, Biggs, S et al. (1 more author) (2015) In situ characterisation of a concentrated colloidal titanium dioxide settling suspension and associated bed development: Application of an acoustic backscatter system. Powder Technology, 284. 530 - 540. ISSN 0032-5910

https://doi.org/10.1016/j.powtec.2015.07.028

In situ characterisation of a concentrated colloidal titanium dioxide settling suspension and associated bed development: Application of an Acoustic Backscatter System

Jaiyana Bux [a, *], Jeff Peakall [b], Simon Biggs [a, 1], Timothy N. Hunter [a]

[a] Institute of Particle Science & Engineering, University of Leeds, Leeds, LS2 9JT, UK

[b] School of Earth and Environment, University of Leeds, Leeds, LS2 9JT, UK

* Corresponding author. Tel: +44 113 343 2543.

E-mail address: pmjbu@leeds.ac.uk (J. Bux).

J.Peakall@leeds.ac.uk (J. Peakall).

eait.dean@uq.edu.au (S.Biggs).

T.N.Hunter@leeds.ac.uk (T.N. Hunter).

[1] Present address: University of Queensland, Brisbane, Qld 4072, Australia

Abstract

The ability to accurately characterise the settling of particulate suspensions is imperative in numerous industries for improved processing, optimisation and control. Characterisation is typically a non-trivial process, and in situ measurements that remove the restriction of requiring particular sample sizes are preferred. Here for the first time, we explore the use of an acoustic backscatter system (ABS) to characterise key settling dynamics within a common colloidal mineral suspension, where backscatter attenuation is heightened due to the associated low scattering cross sections of the particles. Settling titanium dioxide dispersions with concentrations ranging 0.05 – 3.00 vol% were successfully profiled using ABS transducers of 1, 2 and 4 MHz frequencies. This approach enabled the simultaneous visualisation of both the settling interface and sediment bed formation, generating sedimentation curves and eluding settling velocities. Furthermore, backscatter attenuation was empirically correlated with the attenuation-concentration relationship established for homogenous dispersions, to obtain concentration profiles of the settling suspensions. The data depicted concentration changes as a function of time in a hindered settling suspension, and allowed observation of the segregation of a size polydisperse suspension. Data were compared with sedimentation data obtained via two common ex situ bench-scale techniques. Critically, the acoustic backscatter method was validated as a powerful in situ characterisation tool for opaque concentrated heterogeneous dispersions, with the ability to provide concentration density information in conjunction with settling kinetics that is not easily attainable via other methods.

Keywords

Acoustic backscatter, colloidal, sedimentation, characterisation, concentration

1. Introduction

Particulate suspensions and colloidal dispersions are ubiquitous in numerous industries, ranging from pigments, cosmetics, pharmaceutical and foods, to minerals processing and treatment of water, sewage and nuclear waste. Understanding the settling, segregation and bed development behaviours in these typically complex solid-liquid systems is often imperative to process design and efficiency [1]. Although settling generally depends on initial suspension heterogeneity and particle levels, settling can change from a pseudo-constant concentration process to a series of increasing rarefaction fan lines with time [2-4]. Also, if segregation instability leads to a significant gradient in particle density with height, hindered settling will become depth dependent, leading to further complexities with time. Importantly, the actual verification of concentration profiles in settling suspensions is non-trivial. The ability to monitor settling rates, sediment bed evolution and concentration changes (which are essential knowledge for optimizing process design [5, 6]) is typically impeded due to the lack of convenient non-invasive measurement techniques [7].

The characterisation of physically extracted samples is frequently practiced, albeit labour intensive, intrusive and incapable of providing spatial and temporal profiles with ease [8]. Alternative approaches include those analysing the transmission-attenuation response of laser light in sample based devices such as the Lumizier (from Lum GmbH) and Turbiscan (Formulation, SA) [9-11]; however, these ex situ systems are only suitable for small sample analysis of slowly evolving suspensions. In situ devises include light based transmission/backscatter or fluorescence devices [12-18], CCD video analysis [19-23], gamma ray [24, 25] or x-ray CATSCAN [26], and also tomographic techniques which

measure electrical resistance within suspensions [27, 28]. However, a number of these techniques suffer from common limitations to their use, such complicated set-ups that encompass specific vessel requirements (and hence are not suitable for deployment industrially) while many are highly intrusive, or complex and expensive in application [29]. Additionally, many are only suitable for specific particle concentration regimes.

Diagnostic ultrasonic techniques however have proven to surmount such caveats to a practicable extent [1, 30, 31], enabling remote and relatively non-intrusive measurement with subsequently high resolution temporal and spatial profiles of suspended concentration, particle size and settling velocities [32]. Typical instrumentation include ex situ bench scale devices comprising separate transmitter and receiver probes [33-35], and even recent interest in B-scan ultrasound imaging [36]. In situ transceiver devices utilizing Doppler shift measurements provide improved flexibility, such as the ultrasonic velocity profiler which employs only a single frequency [37, 38], while point profiling can be conducted via acoustic Doppler velocimetry [39, 40] and large dilute depths via the acoustic Doppler current profiler [41, 42]. Furthermore, related acoustic backscatter systems (ABS) offer the capability of employing multiple frequencies, and enable minimally intrusive true in situ depth profiling of suspensions without specific sample size requirements [43, 44]. Hence, they can be deployed on a laboratory bench scale or potentially large scale industrial systems.

Acoustic backscatter systems are typically utilised in estuarine sediment transport studies [45], for the characterisation of dilute (<1 g/L) sand suspensions with particles typically tens of microns in size or larger [46]. In this scenario, acoustic backscatter theory can be applied to determine concentration or particle size from measured backscatter intensity data since particle specific backscatter and attenuation properties are known [46]. This approach is inapplicable in concentrated suspensions where increased concentration enhances inter-particle scattering [43] and where small particle radii augment the influence of viscous attenuation on the backscatter signal [47]. Indeed, there is a challenge in characterising suspensions of small particles for which we anticipate a highly attenuated acoustic response. Due to these caveats, it is impossible to apply rigorous theoretical solutions to quantify the backscatter response, although some advances are currently being made to enable determination of the backscatter and attenuation properties of arbitrary particles [48]. Recently, a phenomenological approach has been demonstrated for the characterisation of concentration in non-dilute suspensions (>2.5 g/L) [43, 44] and is applied in this study.

Titanium dioxide was selected in this study owing to its incorporation in numerous consumer products [49]. Its high refractive index renders an opaque suspension, unsuitable for characterisation via optical techniques. Furthermore its fine and cohesive particles readily aggregate, resulting in broad size distributions [1, 50, 51] which is more representative of commonly encountered suspensions. Furthermore at typically 1-2 µm, this acoustically attenuating size is at minimum an order of magnitude smaller relative to traditionally characterised particulate dispersions via acoustic backscatter analysis.

Essentially this paper investigates the capability of a commercially available ABS to characterise a settling, colloidal, industrially relevant mineral suspension. We attempt to identify sludge zone and sediment bed positions, monitor settling dynamics, bed formation, and elucidate potential concentration gradients within polydisperse suspensions. Despite the anticipated challenges, we extend and validate the phenomenological approach for the characterisation of fine colloidal mineral suspensions for the first time here. Indeed we investigate a tool which is insightful with respect to furthering our understanding of the dynamics of polydisperse suspensions, for which theoretical modelling is very much in

development [35, 52, 53], and colloidal cohesive suspensions for which modelling isn't yet well established due to associated complex inter-particle interactions. Moreover this is of direct value where in situ characterisation aids the optimisation of processes involving suspensions.

2. Experimental Procedure

2.1. Materials

All experiments were conducted with an anatase titanium dioxide sample (Degussa, Germany) dispersed in deionized water. Since particle size significantly influences acoustic attenuation and the subsequent measured backscatter response [47], distributions of the dispersed particles prepared via stirring (indicative of the conditions in the proceeding experiments) were obtained via a Malvern Mastersizer 2000 (Malvern Instruments, Worcestershire UK). The average size distribution obtained for three samples which were measured three times over is presented in Fig. 1. For comparative purposes, this is presented alongside the average size distribution of suspensions initially prepared via sonication for the same duration (30 minutes). Essentially, the broader trimodal size distribution of the stirred suspensions illustrates the enhanced level of particle agglomeration encountered within the proceeding experimental suspensions. The median particle diameters (D_{50}) also reflect this, with 7.2 µm for the former and 2.8 µm for the latter.

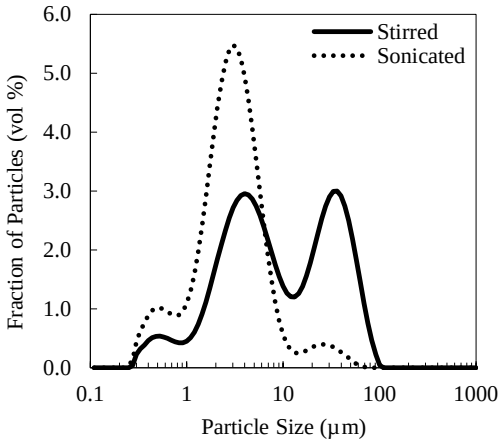

Fig. 1. Particle size distribution comparison (in volume percent) of titanium dioxide dispersions prepared via stirring and sonication

For further validation, the size and shape of the particles were also characterised via scanning electron microscopy (SEM). Dry powder samples were coated with platinum and imaged with a LEO/Zeiss 1530 FEGSEM (LEO Elektronike GmbH, Germany). The images collected at x 2,500 and x 20,000 magnification are respectively presented in Fig. 2. Evidently at lower magnification, Fig. 2(a) depicts a large number of fine particles plus a few relatively larger agglomerates. At higher magnification, Fig. 2(b) suggests that these fines are typically within the 2 µm region with spheroidal structures comprised of aggregated particulates. Currently, the acoustic response of aggregated structures are not well established [54].

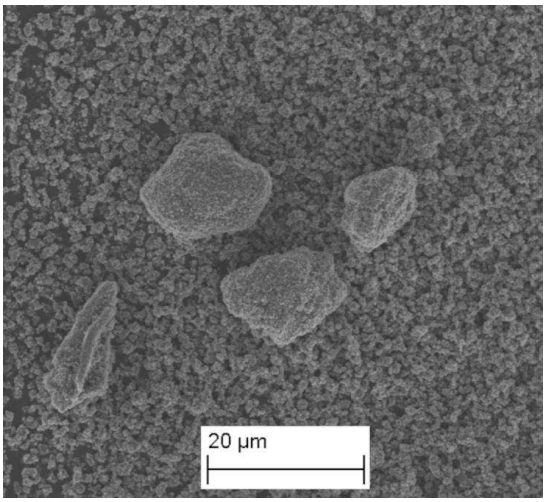

(a)

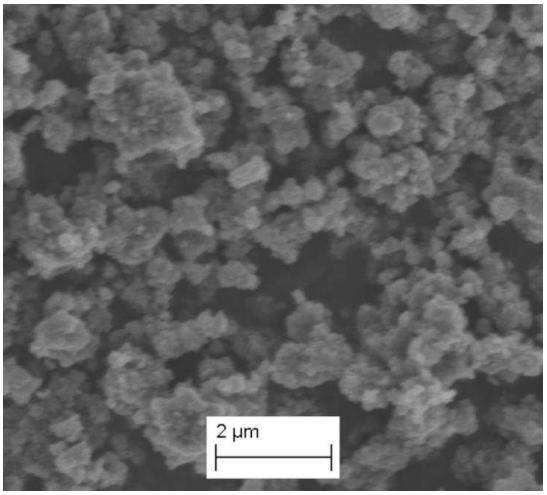

(b)

Fig. 2. Titanium dioxide SEM images at (a) x2,500 magnification, and (b) x20,000 magnification

2.2. In Situ Acoustic Experimental Method

The AQUAscat 1000 ABS (Aquatec Group Ltd, Hampshire, UK) was utilised for experimentation here. It comprises of transceiving probes which propagate selected monochromatic frequencies (0.5 – 5 MHz) into suspension. The active diameters of the transducers range from 1.0 – 1.8 cm depending on frequency. The experimental setup is depicted in Fig. 3. The 1, 2 and 4 MHz transducers were successively submerged below the waterline of a 4 L titanium dioxide – deionised water suspension in a cylindrical Perspex column; 50 cm in height and 10 cm in diameter. Care was taken to degas the suspension via

magnetic stirring prior to experimentation to negate the influence of air bubble attenuation [8]. It was assumed that the speed of sound in the suspension was 1485 ms^{-1}, so close to that in water. The actual value may differ due to the presence of particles in suspension and any air entrainment [8], however it wasn't expected to have significant effect on subsequent measurements. Isonification involved pulse propagation for 4 minutes at 64 Hz. [55, 56]. The measured voltage root mean square backscatter response is converted into the decibel scale ($20\log_{10}(V_{RMS})$ and is referred to as backscatter intensity in proceeding discussions. The measurement output was set at one averaged backscatter profile per second. This represents beyond 1000 sample data recommended by the manufacturer [57]. Since the backscatter intensity is highly dependent upon the medium of interaction, this measurement provides a means of characterising suspension composition [15]. And from the incremental delay in the echo response, suspensions can be characterised depth wise (up to 10 m has been demonstrated in dilute estuarine suspensions [58]). For most measurements in this study, a depth of 0.45 m was profiled and segregated into 2.5 $x10^{-3}$ m bins

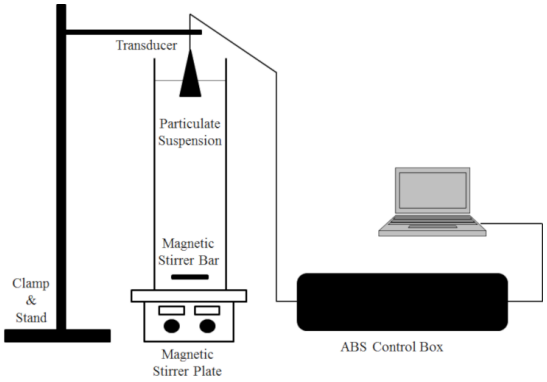

Fig. 3. Experimental system schematic

Initially, a set of calibration experiments were conducted to elucidate the backscatter decay curves of homogenous titanium dioxide suspensions at incremental concentration increases from 0.05 – 3.00 vol% solids concentration, at each frequency, where the particles were suspended continually via a magnetic stirrer bar at 300 rpm. Each experiment was repeated three times. Note an independent concentration test was conducted prior to acoustic investigation to ensure homogenous integrity throughout the 0.45 m depth (see supplementary material). These calibrations critically identified the unique relationship between acoustic attenuation and concentration with respect to isonification frequency, which has not previously been recorded for titanium dioxide suspensions, and provides a reference relationship which can be utilised to characterise concentration from measured backscatter intensity. This approach is advantageous in that direct knowledge of particle specific backscatter and attenuation properties is not a prerequisite for characterisation purposes [6].

Additionally, the ABS was used to characterise settling TiO_2 suspensions.. Specifically 1.1 vol% suspensions, which are expected to be on the cusp of a free settling – hindered settling regime (refer to section 3.2) were selected, to enable measurement without exceeding the concentration limits of the device with respect to signal attenuation effects. This solids concentration is also within the region utilised in personal care products where titanium dioxide concentrations are regulated [49], and concentrations encountered in engineering processes. A 2 MHz frequency probe was selected for the optimisation of signal attenuation

effects versus resolution. Here, the transducer was positioned at 0.18 m from the base of column and a total column suspension height of 0.14 m was measured. These changes were necessitated by the high attenuation of the titanium dioxide dispersions reducing the total acoustic penetration depth at higher particle concentrations. The ABS was set to profile the settling suspension after an initial five minute homogenisation period. The magnetic stirrer was then removed to prevent interference with sediment bed consolidation and backscatter data was collected for a total duration of 15 minutes. For validation purposes, an identical independent settling experiment was conducted in the absence of the ABS. Here 20 ml samples were extracted via syringe and rubber tubing at a position of 0.125 m from the column base (just above the near-bed region). Samples were extracted at 2 minute intervals for a 14 minute settling duration. The samples were weighed wet and dry to determine solids concentration.

2.3. Ex Situ Visual and Laser Characterisation Methods

In order to validate the settling data obtained via the ABS, two ex situ laboratory techniques were employed to obtain comparative settling data. Initially, a traditional settling test was conducted [50] with 1.1, 1.6 and 2.1 vol% titanium dioxide suspensions prepared in 1 L measuring cylinders. The suspensions underwent agitation to ensure uniform mixing via x 15 inversions of the cylinder. Subsequently, the movement of the supernatant – settling suspension interface was measured and timed with a stop watch over a 15 minute duration (by which point bulk settling had ceased). A time value was recorded at every 50 ml graduation during zonal settling and appropriate smaller graduations during compression settling. It was not possible to investigate the settling of a 0.5 vol% suspension in this manner, as it was impossible to observe the demarcation of a clarified settling suspension interface by eye at this concentration.

An additional secondary technique measured light turbidity via the Turbiscan Lab Expert Profiler (Fullbrook Systems, UK). Specifically here, 20 ml sample vials (with a 0.04 m profiling depth) were prepared with 0.5, 1.1, 1.6 and 2.2 vol% suspensions which were agitated for uniformity. The sample vials were consecutively inserted in the instrument and scanned vertically via a laser set at 800 nm. The highest scan rate (2 scans/min) was applied for 10 min duration. The descent of the settling cloud was monitored via laser transmission intensity measurement through the vial, and sediment bed formation via backscatter intensity measurement at 45°. Advantageously, this technique enabled simultaneous visualisation of the evolving settling and sediment bed interfaces even for the lower concentration regime at 0.5 vol%.

3. Results and Discussion

3.1. Attenuation – Concentration Relationship Ascertained in Homogenous Dispersions

Here, the acoustic response of homogenous titanium dioxide dispersions is reported, where the backscatter intensity measured with respect to transducer distance bin, are presented in Fig. 4 (a-c) for 1, 2 and 4 MHz respectively covering 0.05 – 3.00 vol% suspension concentration range. These data depict the mean backscatter intensity over the entire duration of measurement for each homogenous concentration (note, some concentration profiles have been omitted from Fig. 4 for aesthetic reasons). The initial 0.05 m of data, approximately corresponding to the transducers' near-field regions, are also disregarded to avoid signal errors incurred due to complex signal interferences occurring within the region [32]. Additionally, the manufacturer advises that the minimum signal threshold of the AQUAscat

1000 is -72 dB, beyond which there is discontinuity between the acoustic pulse and generated voltage [57]. Thus, all data beyond -70 dB are neglected in data analysis to provide a safety margin.

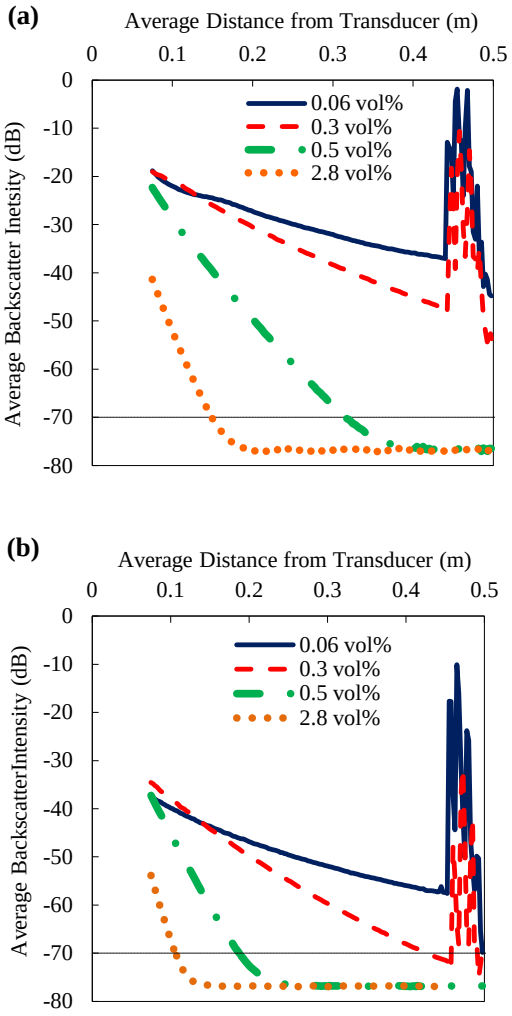

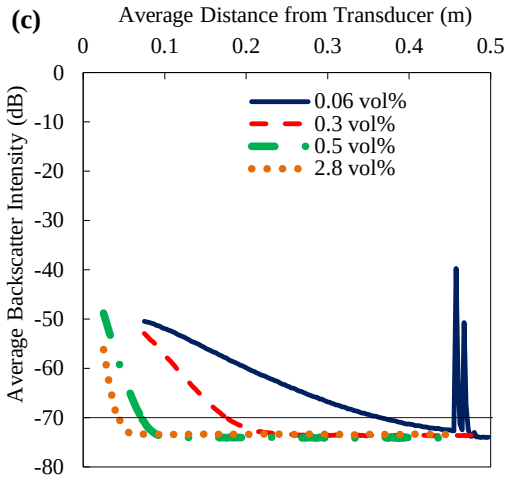

Fig. 4. Homogenous suspension backscatter profiles at (a) 1 MHz, (b) 2 MHz and (c) 4 MHz, where the dashed line at -70 dB represents the signal cut-off threshold

Generally, the backscatter profiles in Fig. 4 display a significant reduction in backscatter intensity with distance, correlating to profiles expected for highly attenuating suspensions. Additionally, some low concentration profiles also display a peak at around 0.45 m corresponding to the experimental column base which behaves as a strong scattering plane. Initially, it was expected that the detection of a measureable backscatter response from these fine particles would be challenging in comparison to larger particle suspensions typically characterised [46] owing to the small scattering cross section inherent in small particles (a significant issue in static backscatter devices and due to the heightened attenuation caused by viscous absorption of submicron particles in addition to scattering losses[47]. Nonetheless, although backscatter intensity and subsequent penetration depth is relatively weaker than that encountered in analogous experiments with larger (40 µm) spherical glass particles (reported by the authors) [43, 44], the intensity in the suspensions here is in fact measurable. With data variability ranging 0.0 – 5.6 dB for the 1 MHz, 0.0 – 1.27 dB for the 2 MHz and 0.0 – 1.03 dB for the 4 MHz transducers, highlighting good consistency within the signal. The highest variability experienced at 1 MHz was at the lower concentrations. Crucially, we have identified that these substantially attenuating colloidal dispersions are indeed still suitable for this type of measurement technique, despite the enhanced concentration and depth penetration limitations.

Additionally, , comparison of Fig. 4 (a-c) reveals that, as expected [59], attenuation is enhanced with increasing frequency,, as the associated shorter wavelength are more susceptible to absorption. This relationship also suggests that increasing the frequency inevitably increases sensitivity to concentration changes, thus improving resolution, and these competing features require some consideration when designing acoustic backscatter experiments, such that a compromise may need to be made between achievable penetration depth and the resolution [41, 43, 44].

Referring back to the profiles in Fig. 4 (a-c), the varying degrees in attenuation with respect to concentration are also apparent. In the lower concentration regimes, the attenuation gradients adhere to a logarithmic decay which progressively resembles linear decay with

increasing concentration. To expand on this observation, the factors which contribute to acoustic backscatter response are presented in the following equation (as summarised by Hunter et al.) [43]:

$$V_{RMS}[dB] = 20log_{10}\left(\frac{K_s K_t C^{½}}{L \Psi}\right) - 40\alpha L \ ,$$

Where the particle backscattering constant Ks, transducer constant Kt, particle concentration C, transducer range L, spherical spreading constant Ψ and combined fluid and particle attenuation constant α are influential. From this relationship we see that there are two major components which contribute to the overall backscatter response; the terms which influence backscattering intensity and the terms influencing attenuation. Collectively, the backscatter component exhibits a logarithmic relationship and the attenuation component exhibits a linear relationship on the dB scale. Hence, when a suspension is dilute, the attenuation factor is less influential and a backscatter profile with a logarithmic decay is expected. However, when attenuation is enhanced in more concentrated regimes, a profile with a linear decay and reduced backscatter intensity is expected [43, 46, 60, 61].

Accordingly, the averaged linear slope of each concentration profile in Fig. 4 (a-c) was calculated for each dispersion and frequency, in order to create an attenuation-concentration correlation. These data are presented in Fig. 5 (a). Evidently, above a certain concentration threshold for each frequency, attenuation appears to follow a linear decay relationship with respect to concentration (illustrated via the dashed lines on Fig. 5 (a)). Below this threshold in the dilute regime, scattering is dominant and a linear relationship is not observed. This is corroborated by the corresponding R^2 analyses presented in Fig. 5 (b), where the dotted line at 0.995 represents the linear threshold taken in this case. The linearity observed at higher concentrations is important, as this demonstrates that a direct non depth dependent correlation can be made between attenuation measurements and concentration, which can be exploited to characterise concentration changes in subsequent concentrated settling titanium dioxide experiments, as well as a future reference for characterising suspensions with analogous particles.

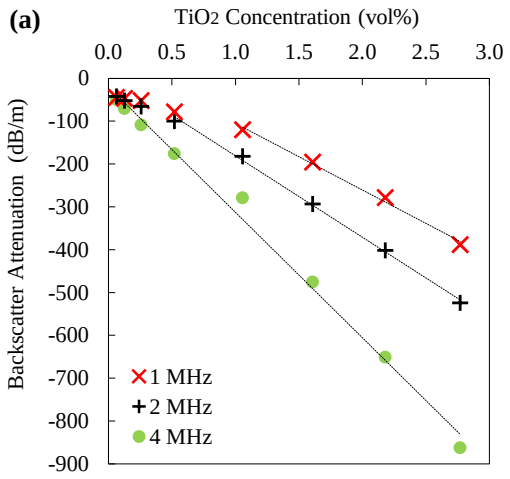

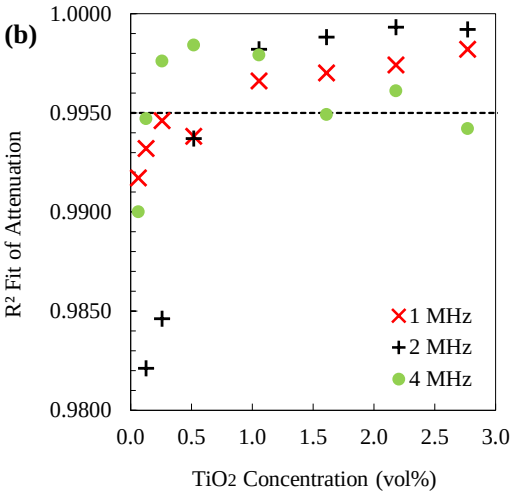

Fig. 5. (a) The attenuation – concentration relationship for all frequencies, where the dashed lines represent a linear trend, and (b) the corresponding attenuation R^2 analysis, i.e. deviation from linear decay, where the dotted line represents the linear threshold.

3.2. Characterising Settling Suspensions; Ex Situ Technique Results

The settling of suspension concentrations ranging 0.5 – 2.2 vol%, measured via the Turbiscan technique are presented in Fig. 6 (a) with the descent of the settling suspension interface as well as the simultaneous formation of a sediment bed at the column base depicted at each concentration. Evidently, all concentrations exhibit an initial zonal hindered settling zone as the clarified supernatant – settling suspension interface descends towards the column base, at constant velocity, followed by a compression settling zone when the suspension interface meets the bed interface. Also, sedimentation is hindered markedly with increasing particulate concentration which enhances fluid drag [62-66]. Additionally, titanium dioxide slurry is known to have strong inter-particle interactions, which could increase hindered settling effects (from changes expected for discrete spheres) [51] and the presence of a wide size range is expected to enhance these interactions [67].

The results of standard timed batch settling tests conducted in measuring cylinders are presented in Fig. 6 (b). Notably, no sediment bed data were measured owing to the lack of contrast hindering observation of the suspension – bed interface. Similarly, it wasn't possible to discern the settling suspension interface by eye at the lowest concentration (0.5 vol%) and the interface was too diffuse owing to the Brownian motion of the colloids in the dilute suspension [68]. Essentially the sedimentation curves obtained in these settling tests bear close resemblance to those obtained via the Turbiscan. Any deviations between the two results are because the Turbiscan only enables depth measurement up to 0.04 m, and thus statistically is much less accurate than the measuring cylinder 0.30 m in height. Furthermore changes in relation to the cylinder could also be down to the small width of the Turbiscan bottles creating wall-effects from wall slip and potentially altered flow lines in relation to the larger settling vessel.

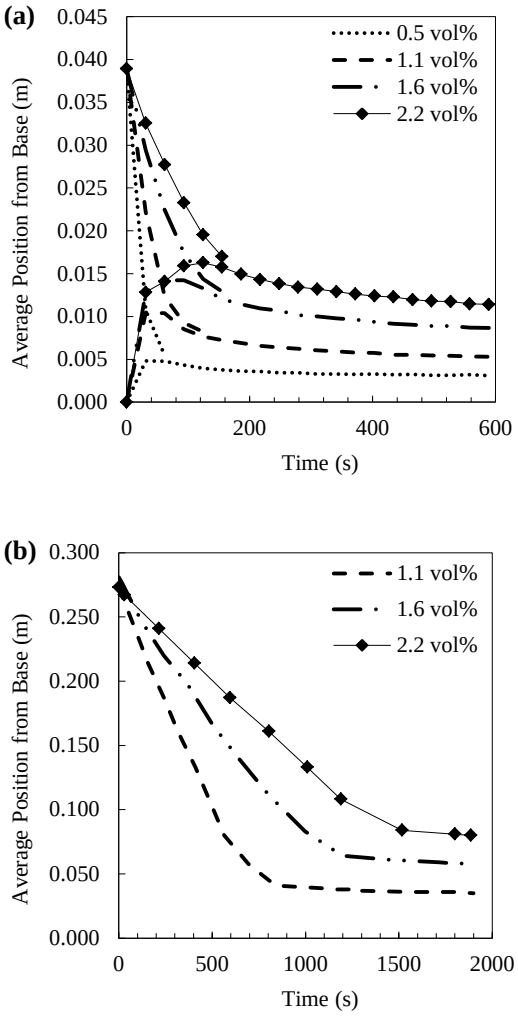

Fig. 6. Sedimentation curves visualising suspension interface demarcation and bed evolution from the base at various concentrations via (a) Turbiscan and (b) measuring cylinder technique.

The bulk suspension settling velocities from the data in Fig. 6 were extracted from the slope of each linear zonal settling region and directly associated against each concentration, and is presented in Fig.7 for both ex situ methods, (note concentration is expressed here in kg/m^3). Variability in the Turbiscan velocities averaging $0.2\text{x}10^{-4}$ m/s and the $0.5\text{x}10^{-4}$ m/s in the measuring cylinders. Both Turbiscan and cylinder data were fitted to an exponential type decay of settling velocity with respect to increasing concentration, analogous to that defined by the Vesilind equation [69, 70], where settling velocity V_1 is calculated from knowledge of the particle free settling velocity V_0, second empirical Vesilind parameter k_1 and particle concentration $\emptyset$;

$$V_I = V_0 e^{-k_1 \emptyset} .$$

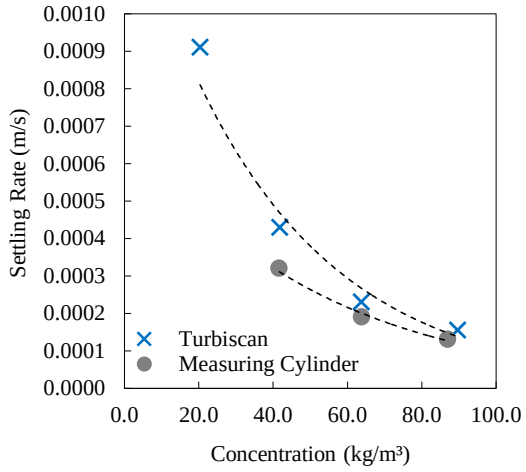

Fig. 7. The influence of concentration on settling rate, determined via Turbiscan and measuring cylinder batch sedimentation (where the dashed lines represent the corresponding Vesilind fits)

Assuming a Vesilind fit of the data in Fig. 7, the data points were extrapolated to obtain estimated particle free settling velocity V_0 (from the zero concentration intercept) and empirical Vesilind parameter k_1 (which correlates to the degree of hindered settling). These are compared in Table 1, with the theoretical Stokes free settling velocity calculated for the titanium dispersion, with (D_{50}) 7.2 µm and a manufacturer density of 3900 kg/m^3. Notably, the Stokes free settling velocity is much lower as calculated from the Stokes relationship than estimated with either Turbiscan or cylinders from the Vesilind intercept. The discrepancy is likely due to differing levels of aggregation in the real experimental systems. As evidenced from Fig. 1, mixing without the use of a sonicator (as conducted for the experimental studies) resulted in a polydisperse suspension with a much higher proportion of larger aggregates, and hence correspondingly higher mean settling velocities than those estimated simply the D_{50}. Also, the Stokes equation considers only discrete spheres not irregular shaped aggregates.

Table 1. Comparison of calculated free settling velocity and Vesilind parameters

	Turbiscan	**Measuring Cylinder**	**Stokes (Theoretical)**
Free Settling Velocity (m/s)	$5x10^{-4}$	$3\ x10^{-4}$	$0.8x10^{-4}$
Vesilind Parameter (m^3/kg)	0.0024	0.0013	_

Comment [TH1]: I think these are the wrong way round, the free settling veolicites are the zero intercept (24 x10-4 and 13 x 10-4) while the other numbers are probably the vesilind parameter

More importantly, Fig. 7 (and the associated hindered fit parameter shown in Table 1) suggests some importance differences in settling behaviour evidenced with the Turbiscan and cylinder tests. It is clear that measured mean settling velocities are higher in all cases with the Turbiscan, while the Vesilind fit parameter is also enhanced (indicating stronger hindering effects with concentration changes). These variations again point to differences in the

aggregation state of suspensions between the two systems, and a likely greater level of agglomeration with the Turbiscan tests. Owing to the time taken to load the small sample vials in the Turbiscan, it appears a level of re-aggregation has occurred that was not broken down with the agitation of the vials before measurement. This highlights the difficulties of using ex situ techniques that require small discrete samples, especially for evaluating the behaviour of aggregated systems. Additionally, the low time resolution of the Turbiscan (2 scans/min) may have also led to a reduction in data quality in respects to the cylinders.

3.3. Characterising Settling Suspensions; In Situ Acoustic Results

3.3.1. Sedimentation Behaviour and Concentration Changes

The backscatter data from the 2 MHz settling experiments were recorded in time profiles. Although one depth profile was recorded every second, the data were smoothed by taking 5 s and 5 distance bin moving averages to reduce the effects of inherent noise from random fluctuations within the dynamic settling system [71]. This essentially achieves smoothing of the data for analysis in a short enough time frame that any significant changes in the settling suspension are still observed. A selection of smoothed backscatter profiles from the settling experiments are presented in Fig. 8 (a-f). A range of time frames which illustrate the overall evolution of the settling suspension are exhibited. Note that the peak represented with a dotted line at approximately 0.16 m, is in line with the location of the column base in these experiments.

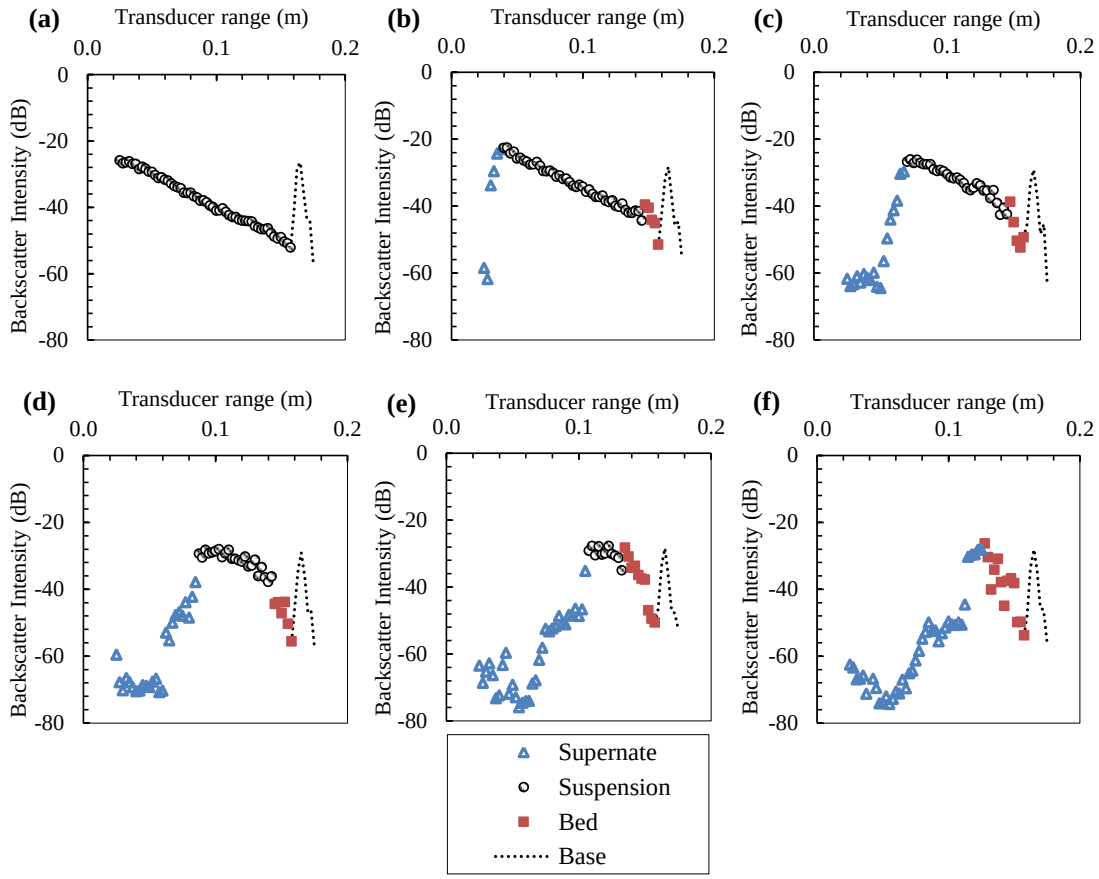

Fig. 8. Evolution of average backscatter profiles with time at (a) 3 s, (b) 143 s, (c) 248 s, (d) 318 s, (e) 388 s, (f) 423 s

The first profile in Fig 8.(a), portrays the moments proceeding measurement initiation, and is reminiscent of a typical backscatter profile for a concentrated homogenous dispersion, (similar to Fig. 4(b)), whereby a linear backscatter decay is proceeded by a peak (dotted line) representing the column base. A homogenous suspension profile at this early stage is consistent with a well-mixed dispersion expected prior to the onset of settling. The second profile approximately at 2.5 minutes (Fig. 8(b)) portrays the formation of three distinct regions within the suspension. In the first region (i.e. closest to the transducer), a very weak backscatter response is obtained implying that there are very few particle scatterers in suspension, corresponding with the clarified supernatant region. Subsequently, this supernate region is succeeded with a backscatter peak, after which the intensity decays in a linear fashion, akin to that of a homogenous dispersion. This peak in backscatter intensity is the result of an interaction with a strong scattering plane at the supernatant-suspension boarder. Over time, from Fig. 8(c-e), we observe the gradual shift of this peak further down the experimental column, as expected for a hindered settling system. Interestingly, the linearity of the backscatter decay in the hindered suspension zone k, appears to deviate over time, see Fig. 8 (b-e) and is particularly noticeable in Fig. 8 (d). This suggests a gradual reduction in suspension homogeneity, likely due to particle segregation in the suspension system which comprises a broad size distribution. This observation is consistent with the batch settling of

polydisperse suspensions with a wide distribution, where particles of different sizes segregate and the larger aggregated particles settle out expeditiously [67, 72-74]. Markedly here we have identified the potentially complex settling behaviour of this suspension system from brief observation of the evolving backscatter profiles.

The third notable region of interest is the fluctuation in backscatter intensity exhibited in the near-base vicinity. Initially in Fig 8(b), there is a slight rise in intensity, signifying the formation of a boundary below the zonal settling region. In due course, from Fig. 8 (c-f) that boundary gradually shifts away from the base, i.e. increases in depth. This observation is in line with the formation of a sediment bed in the near-base vicinity, which initially increases in depth. Indeed a compressed bed depth of 0.025 m was physically measured upon experimental completion which coincides well with bed depth visualised in the latter profile Fig. 8(f). Some difficulty was encountered in gauging the exact location of the boundary between the zonal settling and sediment bed regions. Inherently the demarcation lines of inter zone boundaries within settling polydisperse suspensions are not always sharp [75]. This observation indicates the presence of a high-concentration zone directly above the bed (termed the supersediment zone or the rarefaction fan in mathematical models), which is essentially a transition zone between the settling suspension and bed [2, 76].

Error bars were omitted from these averaged profiles for aesthetic reasons, however typical variability in these data for different averaging times was calculated. Initially, the average standard deviation was determined where a continuous average was taken of the profiles in 5 s segments. Accordingly, the variation is in the region of ± 3.9% of backscatter signal in dB. Comparatively, the average variation in the data where 10 s averaging was conducted is ± 4.5%. This increased variability is owed to the kinetic changes in settling suspension interface over time. When 1 s profiles were smoothed over 5 distance bin the average error was (± 10.1%), which in this case is due to the noise level in the system. Thus the challenge is to ensure that the data is sufficiently smoothed such that the influences of inherent noise are negated whilst enabling the timely observation of kinetic changes within the settling suspension. To convert the measured attenuation to concentration, the calibration relationship for 2 MHz was used (Fig. 5). Here, the attenuation was quantified as the gradient between each consecutive 5 distance bin segment, and then correlated with concentration via the reference relationship. A selection of resulting concentration profiles, are presented in Fig. 9(a-f). Similarly to the previous qualitative analysis, we identify that the initial settling suspension is fairly uniform and corresponds with the initial dispersion concentration around 1.1 vol% (Fig. 9(a-b)). As time elapses (Fig. 9(c-f)), the concentration continually increases downwards in a smooth transition indicating the presence of a supersediment or rarefaction fan in a hindered settling system [2, 76]. Although initial concentration is uniform, hindered settling can lead to complicated sedimentation behaviour especially in polydisperse suspensions where different sized particles sediment at different velocities, although generally maximum flux remains constant until the largest particle class has settled settle out [33, 74]. Essentially by 5 minutes (Fig. 9(f)), the concentration at the near-bed boundary is significantly greater than the initial concentration, whilst that in the upper region (near the supernate boundary) falls below the initial suspension concentration of Fig. 9(a). This phenomenon is a consequence of the reduction in the settling velocity of the smaller particle class [2, 53]. These findings are consistent with other experimental investigations of multisized non-colloidal suspensions [2, 22, 43, 44]. Importantly, they demonstrate the ABS's capability for very detailed in situ characterisation of complex sedimentation processes within colloidal polydisperse suspensions. These data are difficult to obtain via

other methods especially via in situ devices, and correspond well qualitatively with previous literature looking at modelled settling trends of polydisperse suspensions [53, 74].

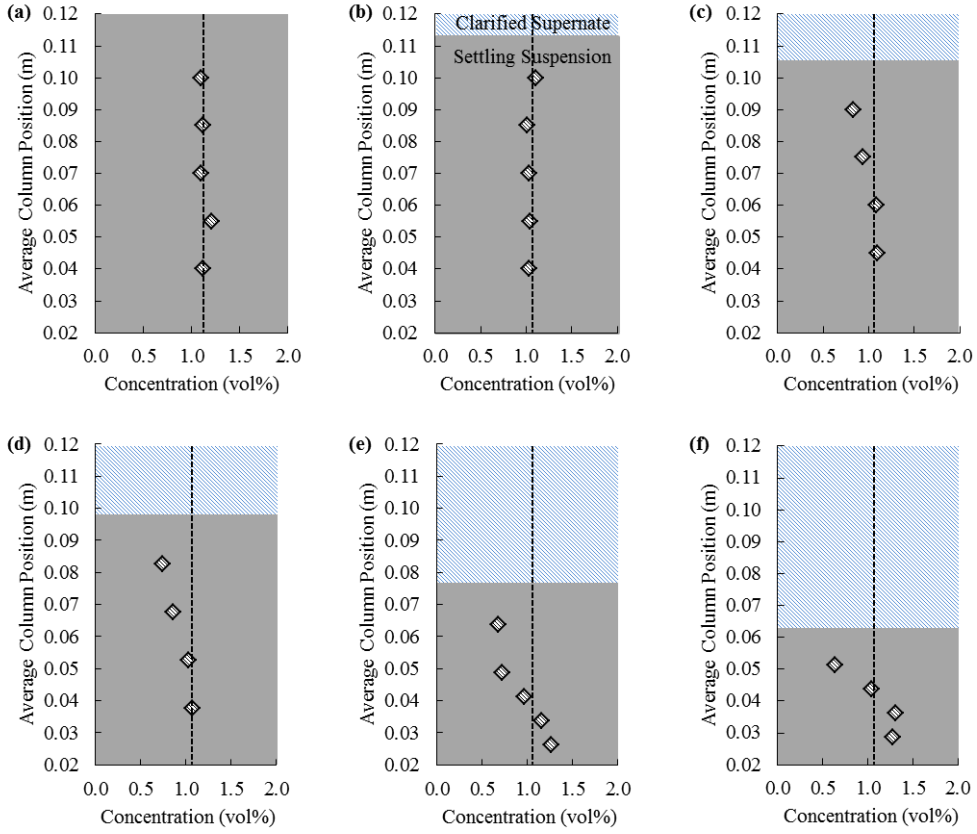

Fig. 9. Settling suspension concentration profiles at (a) 38 s, (b) 143 s, (c) 178 s, (d) 213 s, (e) 283 s and (f) 318 s

3.3.2. Combined concentration and interface phase settling diagram

Thus far we have established that it is possible to track both the settling interface movement as well as concentration changes during the settling process, as demonstrated in Fig. 9(a-f). However this figure only represents selected time intervals. Therefore, the raw scattering data was analysed over every 5 s time-step to present a combined phase diagram for the continuously measured process. Fig. 10 depicts the moving averages of the concentration profiles over distance and time (as discussed in the previous section). Concentration changes are depicted via a colour scale; light to dark representing dilute to concentrated regimes respectively. It is clear from Fig. 10 that the level of noise associated with individual time-steps from the measured backscatter signal is relatively high. Nonetheless, it is indeed possible to identify the delineation of a clarified supernatant – settling suspension interface, alongside the gradual development of a high concentration near-bed zone that is denoted by the concentration increase in the near-base region (the actual sediment bed is just below the viable image).. Crucially, this highlights that the ABS is capable of providing a substantially deeper level of information on the dynamics of a settling suspension on a real time basis in

comparison to other techniques such as the Turbiscan, which only provide settling interface data. The ABS can provide specific depth-wise concentration data provided a reference attenuation – concentration relationship is available. Where a reference is not available, a colour plot akin to Fig. 11, conveying changes in attenuation levels rather than the given concentration, would provide a somewhat qualitative indication of inner suspension characteristics in conjunction with a sedimentation curves.

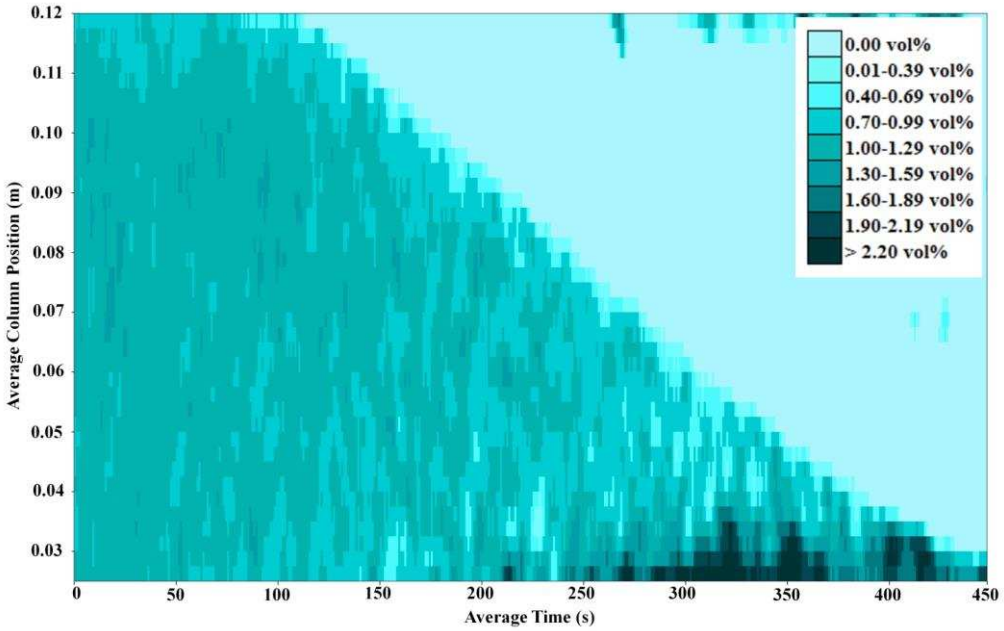

Fig. 10. Combined concentration settling interface phase diagram

In order to compare the sedimentation behaviour directly with those obtained via the Turbiscan and measuring cylinder techniques, a sedimentation curve analogous to those in Fig. 6(a-b) is presented in Fig. 11. Here 30 s smoothed time averages were taken and similarly selected concentration profiles were separated into regions of 0.51 – 0.70, 0.71 – 0.90, 0.91 – 1.10 and 1.11 – 1.30 vol%, where the upper peak was directly plotted as the settling interface and lower signal peak plotted as the consolidated bed boundary. . For comparative purposes, the linear gradient of the zonal settling regions in the 1.1 vol% settling suspensions from Fig. 6(a-b) and Fig. 11 were calculated and summarised in Table 2. The measured ABS and cylinder velocities are identical ($3x10^{-4}$ m/s) providing confidence in the ABS's ability to accurately measure settling kinetics, while the Turbiscan settling rate of $4x10^{-4}$ m/s is slightly more rapid in comparison. It must be noted that the Turbiscan experiments were conducted in much smaller (20 ml) sample vials enabling only 0.04 m of measurement depth at a maximum scan rate of 2 scan/min. Here bulk settling was complete within three scans (i.e. three data points), thus little settling data were retrieved. Consequently, it is expected that statistically the greatest level of error will have been incurred with this laser method.

By presenting the averaged ABS settling data as shown in Fig. 11, the capabilities of this instrumentation technique are fully observed. Notably, the ABS enabled simultaneous visualisation of settling kinetics, bed evolution and detailed concentration changes, even in

micron sized colloidal dispersions at the limit of backscattering detection, due to the small cross sectional area and absorptive attenuation. Importantly, a low concentration zone in the upper suspension is clearly evident, suggesting segregation of the finer particles from the bulk. This behaviour essentially indicates that even at 1.1 vol%, concentrations are not great enough for the settling to occur completely en masse as would be expected for strongly hindered dispersions. While such density information in conjunction with settling kinetics, is either not possible or easy attainable via other methods, the main advantage of the ABS is that it can be used in situ. This allows measurements that are independent of the sample cell, allowing large cylinders to be used for settling, overcoming issues with small sample preparation as evidenced with the Turbiscan. .

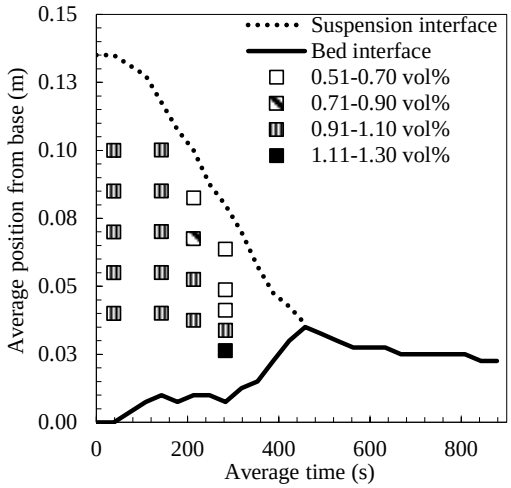

Fig. 11. 1.1 vol% TiO_2 settling phase diagram, as measured with the ABS (incorporating average concentration changes)

Table 2. Settling velocities of 1.1 vol% titanium dioxide dispersions obtained via three techniques

Technique	Settling Velocity (m/s)
ABS	$3x10^{-4}$
Measuring Cylinder	$3x10^{-4}$
Turbiscan	$4x10^{-4}$

4. Conclusion

An acoustic backscatter system was deployed to characterise sedimentation processes and concentration density changes in a settling titanium dioxide suspension. Characterisation of a concentrated colloidal mineral suspension for which the backscatter and attenuation coefficients are unknown, was demonstrated for the first time here via an empirical analysis approach. Initially the backscatter attenuation was quantified in homogenous titanium dioxide dispersions ranging from 0.05 – 3.00 vol% in concentration. Consequently a linear

relationship was established between the two parameters at 1, 2 and 4 MHz frequencies. Subsequently a settling titanium dioxide suspension was profiled at 2 MHz, where the calibrated attenuation – concentration relationship was exploited to characterise concentration changes in the settling suspension. Interestingly the results indicated the gradual development of a downward concentration gradient whereby the concentration at the supernate – suspension boundary dropped below the initial concentration, and a concentrated supersediment formed in the near-base region. Moreover the ABS also enabled simultaneous visualisation of both settling interface and sediment bed evolution over time, from which settling rates were extracted and hindered settling behaviour was inferred. These data compared well with that extracted from ex situ laboratory experiments.

To conclude the ABS captured very complicated sedimentation behaviour in a polydisperse colloidal settling suspension, for which mathematical methods and ex situ batch scale experiments are normally required to predict behaviour. We have demonstrated an in situ measurement technique that can visualise intricate interior dynamics in batch scale lab experiments. Furthermore since the device comprises of a single transceiving probe, it offers versatility in terms of application, i.e. it is very flexible for deployment in field applications [52]. On a final note, since concentration will denote some restrictions with respect to achievable penetration depth in commercial devices, future work also involves the development of an enhanced instrument design which aims to achieve desired penetration depths of up to a few meters for application in industry, without compromising resolution for detailed concentration analysis.

Acknowledgements

The authors would like to thank the EPSRC and the Nuclear Decommissioning Authority (NDA) for funding this research, and Dave Goddard of the National Nuclear Laboratory for supervisory support on behalf of the NDA. Furthermore, the authors would like to thank Sellafield Ltd for industrial consultation regarding this project and Nabeel Bux for valuable input regarding data analysis.

References

[1] R.E. Challis, M.J.W. Povey, M.L. Mather, A.K. Holmes, Ultrasound techniques for characterizing colloidal dispersions, Reports on Progress in Physics, 68 (2005) 1541-1637.
[2] R. Dorrell, A.J. Hogg, Sedimentation of bidisperse suspensions, International Journal of Multiphase Flow, 36 (2010) 481-490.
[3] S.P. Usher, L.J. Studer, R.C. Wall, P.J. Scales, Characterisation of dewaterability from equilibrium and transient centrifugation test data, Chemical Engineering Science, 93 (2013) 277-291.
[4] R. Holdich, Fundamentals of Particle Technology, Midland Information Technology and Publishing, Nottingham, 2009.
[5] J. De Clercq, I. Nopens, J. Defrancq, P.A. Vanrolleghem, Extending and calibrating a mechanistic hindered and compression settling model for activated sludge using in-depth batch experiments, Water Research, 42 (2008) 781-791.
[6] E. Iritani, T. Hashimoto, N. Katagiri, Gravity consolidation–sedimentation behaviors of concentrated TiO2 suspension, Chemical Engineering Science, 64 (2009) 4414-4423.
[7] M.K. Cheung, R.L. Powell, M.J. McCarthy, Sedimentation of noncolloidal bidisperse suspensions, Aiche Journal, 42 (1996) 271-276.
[8] R. Meral, Laboratory Evaluation of Acoustic Backscatter and LISST Methods for Measurement of Suspended Sediments, Sensors, (2008) 979-993.

[9] T.N. Hunter, J. Peakall, S.R. Biggs, Ultrasonic velocimetry for the in situ characterisation of particulate settling and sedimentation, Minerals Engineering, 24 (2011) 416-423.
[10] N. Paul, S. Biggs, M. Edmondson, T.N. Hunter, R.B. Hammond, Characterising highly active nuclear waste simulants, Chemical Engineering Research and Design, 91 (2013) 742-751.
[11] T. Sobisch, D. Lerche, Thickener performance traced by multisample analytical centrifugation, Colloids and Surfaces A: Physicochemical and Engineering Aspects, 331 (2008) 114-118.
[12] B.L. Finlayson, Field calibration of a recording turbidity meter, CATENA, 12 (1985) 141-147.
[13] D.M. Lawler, R.M. Brown, A simple and inexpensive turbidity meter for the estimation of suspended sediment concentrations, 6 (1992) 159-168.
[14] J.F. Lynch, J.D. Irish, C.R. Sherwood, Y.C. Agrawal, Determining suspended sediment particle size information from acoustical and optical backscatter measurements, Continental Shelf Research, 14 (1994) 1139-1165.
[15] D.C. Fugate, C.T. Friedrichs, Determining concentration and fall velocity of estuarine particle populations using ADV, OBS and LISST, Continental Shelf Research, 22 (2002) 1867-1886.
[16] J.W. Gartner, R.T. Cheng, P.-F. Wang, K. Richter, Laboratory and field evaluations of the LISST-100 instrument for suspended particle size determinations, Marine Geology, 175 (2001) 199-219.
[17] Y.C. Agrawal, H.C. Pottsmith, Instruments for particle size and settling velocity observations in sediment transport, Marine Geology, 168 (2000) 89-114.
[18] R. Styles, Laboratory evaluation of the LISST in a stratified fluid, Marine Geology, 227 (2006) 151-162.
[19] J.M. Fan, Z. Cui, Effect of Acoustic Standing Wave in a Bubble Column, Industrial & Engineering Chemistry Research, 44 (2005) 7010-7018.
[20] R. Lau, M.S. Hassan, W. Wong, T. Chen, Revisit of the Wall Effect on the Settling of Cylindrical Particles in the Inertial Regime, Industrial & Engineering Chemistry Research, 49 (2010) 8870-8876.
[21] M.V. Sardeshpande, V.V. Ranade, Simulation of Settling of Solid Particles Due to Sudden Impeller Stoppage, Industrial & Engineering Chemistry Research, 51 (2012) 4112-4118.
[22] L. Hernando, A. Omari, D. Reungoat, Experimental study of sedimentation of concentrated mono-disperse suspensions: Determination of sedimentation modes, Powder Technology, 258 (2014) 265-271.
[23] L. Hernando, A. Omari, D. Reungoat, Experimental investigation of batch sedimentation of concentrated bidisperse suspensions, Powder Technology, 275 (2015) 273-279.
[24] J. WHEELER, S. CHATTERJI, Settling of Particles in Fresh Cement Pastes, Journal of the American Ceramic Society, 55 (1972).
[25] D.R. Kaushal, Y. Tomita, Experimental investigation for near-wall lift of coarser particles in slurry pipeline using γ-ray densitometer, Powder Technology, 172 (2007) 177-187.
[26] C.P. Chu, S.P. Ju, D.J. Lee, F.M. Tiller, K.K. Mohanty, Y.C. Chang, Batch Settling of Flocculated Clay Slurry, Industrial & Engineering Chemistry Research, 41 (2002) 1227-1233.
[27] F. Dickin, M. Wang, Electrical resistance tomography for process applications, Measurement Science and Technology, 7 (1996).

[28] G.T. Bolton, M. Bennett, M. Wang, C. Qiu, M. Wright, K.M. Primrose, S.J. Stanley, D. Rhodes, Development of an electrical tomographic system for operation in a remote, acidic and radioactive environment, Chemical Engineering Journal, 130 (2007) 165-169.
[29] A. Shukla, A. Prakash, S. Rohani, Particles settling studies using ultrasonic techniques, Powder Technology, 177 (2007) 102-111.
[30] R.A. Williams, C.G. Xie, R. Bragg, W.P.K. Amarasinghe, Experimental techniques for monitoring sedimentation in optically opaque suspensions, Colloids and Surfaces, 43 (1990) 1-32.
[31] J.R. Gray, J.W. Gartner, Technological advances in suspended-sediment surrogate monitoring, Water Resources Research, 45 (2009).
[32] A. Downing, P.D. Thorne, C.E. Vincent, Backscattering from a suspension in the near field of a piston transducer, The Journal of the Acoustical Society of America, 97 (1995) 1614-1620.
[33] M. Hoyos, J. Bacri, J. Martin, D. Salin, A study of the sedimentation of noncolloidal bidisperse, concentrated suspensions by an acoustic technique, Physics of Fluids (1994-present), 6 (1994) 3809-3817.
[34] P.V. Nelson, M.J.W. Povey, Y. Wang, An ultrasound velocity and attenuation scanner for viewing the temporal evolution of a dispersed phase in fluids, Review of Scientific Instruments, 72 (2001) 4234-4241.
[35] A. Deboeuf, G. Gauthier, J. Martin, D. Salin, Segregation and periodic mixing in a fluidized bidisperse suspension, New Journal of Physics, 13 (2011) 075005.
[36] X.-j. Zou, Z.-m. Ma, X.-h. Zhao, X.-y. Hu, W.-l. Tao, B-scan ultrasound imaging measurement of suspended sediment concentration and its vertical distribution, Measurement Science and Technology, 25 (2014) 115303.
[37] T. Hunter, J. Peakall, S. Biggs, Ultrasonic velocimetry for the< i> in situ</i> characterisation of particulate settling and sedimentation, Minerals Engineering, 24 (2011) 416-423.
[38] J.F. Stener, J.E. Carlson, B.I. Pålsson, A. Sand, Evaluation of the applicability of ultrasonic velocity profiling in conditions related to wet low intensity magnetic separation, Minerals Engineering, 62 (2014) 2-8.
[39] S.N. Lane, P.M. Biron, K.F. Bradbrook, J.B. Butler, J.H. Chandler, M.D. Crowell, S.J. McLelland, K.S. Richards, A.G. Roy, Three-dimensional measurement of river chnnel flow processes using Acoustic Doppler Velocimetry, Earth Surface Processes and Landforms, 23 (1998).
[40] H.K. Ha, W.Y. Hsu, J.P.Y. Maa, Y.Y. Shao, C.W. Holland, Using ADV backscatter strength for measuring suspended cohesive sediment concentration, Continental Shelf Research, 29 (2009) 1310-1316.
[41] J.W. Gartner, Estimating suspended solids concentrations from backscatter intensity measured by acoustic Doppler current profiler in San Francisco Bay, California, Marine Geology, 211 (2004) 169-187.
[42] J.L. Best, R.A. Kostaschuk, J. Peakall, P.V. Villard, M. Franklin, Whole flow field dynamics and velocity pulsing within natural sediment-laden underflows, Geology, 33 (2005) 765-768.
[43] T.N. Hunter, L. Darlison, J. Peakall, S. Biggs, Using a multi-frequency acoustic backscatter system as an in situ high concentration dispersion monitor, Chemical Engineering Science, 80 (2012) 409-418.
[44] T.N. Hunter, J. Peakall, S. Biggs, An acoustic backscatter system for in situ concentration profiling of settling flocculated dispersions, Minerals Engineering, 27–28 (2012) 20-27.

[45] C.P. Rose, P.D. Thorne, Measurements of suspended sediment transport parameters in a tidal estuary, Continental Shelf Research, 21 (2001) 1551-1575.
[46] P.D. Thorne, C.E. Vincent, P.J. Hardcastle, S. Rehman, N. Pearson, Measuring suspended sediment concentrations using acoustic backscatter devices, Marine Geology, 98 (1991) 7-16.
[47] S.A. Moore, J. Le Coz, D. Hurther, A. Paquier, Using multi-frequency acoustic attenuation to monitor grain size and concentration of suspended sediment in rivers, The Journal of the Acoustical Society of America, 133 (2013) 1959-1970.
[48] H.P. Rice, M. Fairweather, T.N. Hunter, B. Mahmoud, S. Biggs, J. Peakall, Measuring particle concentration in multiphase pipe flow using acoustic backscatter: Generalization of the dual-frequency inversion method, The Journal of the Acoustical Society of America, 136 (2014) 156-169.
[49] A. Weir, P. Westerhoff, L. Fabricius, K. Hristovski, N. von Goetz, Titanium Dioxide Nanoparticles in Food and Personal Care Products, Environmental Science & Technology, 46 (2012) 2242-2250.
[50] S.W. Bodman, Y.T. Shah, M.C. Skriba, Settling of Flocculated Suspensions of Titanium Dioxide and Alum Mud in Water, Industrial & Engineering Chemistry Process Design and Development, 11 (1972) 46-52.
[51] R.M. Turian, T.W. Ma, F.L.G. Hsu, D.J. Sung, Characterization, settling, and rheology of concentrated fine particulate mineral slurries, Powder Technology, 93 (1997) 219-233.
[52] R. Dorrell, A. Hogg, D. Pritchard, Polydisperse suspensions: Erosion, deposition, and flow capacity, Journal of Geophysical Research: Earth Surface, 118 (2013) 1939-1955.
[53] R. Bürger, R. Donat, P. Mulet, C.A. Vega, Hyperbolicity analysis of polydisperse sedimentation models via a secular equation for the flux Jacobian, SIAM Journal on Applied Mathematics, 70 (2010) 2186-2213.
[54] I.T. MacDonald, C.E. Vincent, P.D. Thorne, B.D. Moate, Acoustic scattering from a suspension of flocculated sediments, Journal of Geophysical Research: Oceans, 118 (2013) 2581-2594.
[55] T.J. Mason, Practical Sonochemistry: user's guide to applications in chemistry and chemical engineering, 1991.
[56] Met-Flow, UVP monitor model UVP-Duo with software version 3. Revision 5 ed., Met-Flow SA, Lausanne, Switzerland, 2002.
[57] A.M. Smerdon, S.M. Simmons, Testing the Limits of a Multi-Frequency Acoustic Sediment Profiling Instrument, Underwater Acoustic Measurements - 3rd International Conference & Exhibition SeriesNafplion, Greece, 2009.
[58] S.A. Moore, G. Dramais, P. Dussouillez, J. Le Coz, C. Rennie, B. Camenen, Acoustic measurements of the spatial distribution of suspended sediment at a site on the Lower Mekong River, ASA, Montreal, Canada, 2013, pp. 005003-005009.
[59] S. Temkin, Suspension Acoustics: An Introduction of the Physics of Suspensions, Cambridge University Press2005.
[60] P.D. Thorne, P.J. Hardcastle, R.L. Soulsby, ANALYSIS OF ACOUSTIC MEASUREMENTS OF SUSPENDED SEDIMENTS, Journal of Geophysical Research-Oceans, 98 (1993) 899-910.
[61] P.D. Thorne, D.M. Hanes, A review of acoustic measurement of small-scale sediment processes, Continental Shelf Research, 22 (2002) 603-632.
[62] E.C. McRoberts, J.F. Nixon, A theory of soil sedimentation, Canadian Geotechnical Journal, 13 (1976) 16.
[63] R.G. Holdich, G. Butt, Solid/liquid separation by sedimentation, Proceedings of the Institute of Mechanical Engineers, Part E: Journal of Process Mechanical Engineering, 211 (1997) 10.

[64] M.D. Green, K.A. Landman, R.G. de Kretser, D.V. Boger, Pressure Filtration Technique for Complete Characterization of Consolidating Suspensions, Industrial & Engineering Chemistry Research, 37 (1998) 4152-4156.
[65] R.H. Davis, K.H. Birdsell, Hindered settling of semidilute monodisperse and polydisperse suspensions, AIChE J., 34 (1988).
[66] R.H. Davis, H. Gecol, Hindered settling function with no empirical parameters for polydisperse suspensions, AIChE J., 40 (1994).
[67] M.S. Selim, A.C. Kothari, R.M. Turian, Sedimentation of multisized particles in concentrated suspensions, Aiche Journal, 29 (1983) 1029-1038.
[68] R. Davis, K. Birdsell, Hindered settling of semidilute monodisperse and polydisperse suspensions, Aiche Journal, 34 (1988) 123-129.
[69] P.A. Vesilind, Design of prototype thickeners from batch settling tests, Water Sewage Works, 115 (1968) 302-307.
[70] C.M. Bye, P.L. Dold, Evaluation of correlations for zone settling velocity parameters based on sludge volume index-type measures and consequences in settling tank design, Water environment research, (1999) 1333-1344.
[71] S.S. Rehman, C.E. Vincent, Underwater acoustic measurement of suspended sediments: the calibration of a high-frequency acoutic backscatter meter, Geol. Bull.Univ. Peshawar, 1990, pp. 161-173.
[72] A.S. Michaels, J.C. Bolger, Settling Rates and Sediment Volumes of Flocculated Kaolin Suspensions, Industrial & Engineering Chemistry Fundamentals, 1 (1962) 24-33.
[73] C. Nadiv, R. Semiat, Batch Settling of Liquid-Liquid Dispersion, Industrial & Engineering Chemistry Research, 34 (1995) 2427-2435.
[74] R. Dorrell, A. Hogg, E. Sumner, P. Talling, The structure of the deposit produced by sedimentation of polydisperse suspensions, Journal of Geophysical Research: Earth Surface (2003–2012), 116 (2011).
[75] K. Stamatakis, C. Tien, Dynamics of batch sedimentation of polydispersed suspensions, Powder Technology, 56 (1988) 105-117.
[76] D.K. Basson, S. Berres, R. Bürger, On models of polydisperse sedimentation with particle-size-specific hindered-settling factors, Applied mathematical modelling, 33 (2009) 1815-1835.